JOURNAL OF MATERIALS SCIENCE 18 (1983) 1751–1757

Analysis of oxalate coating on steels by conversion electron Mössbauer spectrometry

KIYOSHI NOMURA, YUSUKE UJIHIRA
Faculty of Engineering, University of Tokyo, Hongo 7-3-1, Bunkyo-ku, Tokyo 113, Japan

Mild and stainless steels were treated in an oxalate bath for surface finishing and the chemical states of the iron species, produced in the oxalate coating, were investigated using conversion electron Mössbauer spectrometry. The quadrupole splitting of the iron (II) oxalate produced on the stainless steel was slightly smaller than that of the iron (II) oxalate on mild steel. The chemical states of the deposited iron (II) oxalate on both steels were not affected by rolling, although a large part of the oxalate coating on mild steel was easily stripped off by the process. It was found that surface conditioning of stainless steel by oxalate was more effective than that of mild steel, and that the different states of FeC_2O_4 were formed as a thermal decomposition product by the different thermal treatment. The thermal property of oxalate coating was similar to that of $FeC_2O_4 \cdot 2H_2O$. The oxalate coating is concluded to work as a good lubricant rather than a corrosion-resistant material, especially at the surface of stainless steel.

1. Introduction

To date, we have studied the chemical state of iron compounds deposited at the steel surface by the treatment of steels. The chemical state and the epitaxial growth of iron compounds produced on the steel surface by zinc phosphatings were analysed using conversion electron Mössbauer spectrometry (CEMS) [1, 2]. The effect of thermal deterioration of zinc phosphate coatings [3, 4], the thermal decomposition of phosphophyllite [5], variation of chemical composition of the manganese phosphate coating [6], and the site distribution of iron (II) in iron (II) substituted hureaulite [7] were studied by CEMS and conventional transmission Mössbauer spectrometry (TMS). The surface layer structures of the borided, carburized, and nitrided steels were also investigated by CEMS [8–10].

The oxalate coating does not work as well as a protective layer against the corrosion of mild steel and has a poor resistance to thermal deterioration. It is also poor in the adhesion to substrate compared with phosphate coatings [11]. Nevertheless, the oxalate treatment is widely applied to stainless steel as a means of reducing the friction when the steel undergoes plastic deformation and of serving the coating as an appropriate surface lubrication.

In this paper, the characterization of oxalate coatings of mild and stainless steels and the effect of rolling on the variation of the iron state in the coatings are described. The thermal property of coatings and the Mössbauer parameters of the pyrolysis products of iron (II) oxalate dihydrate, $FeC_2O_4 \cdot 2H_2O$, were also studied to identify the iron compounds in the oxalate coatings.

The range of low energy electrons in oxalate coating estimated by applying Feldman's equation [12] to $FeC_2O_4 \cdot 2H_2O$ ($\rho = 2.28$) was R (nm) = $3.88\,E(\text{keV})^{2.77}$. Therefore, the ranges of 7.3 keV (79%) K-, 13.6 keV (8%) L-conversion and 5.5 keV (63%) Auger electrons emitted by the internal conversion process of the excited ^{57}Fe nucleus after resonant absorption of 14.4 keV (100%) γ-rays are 955, 5350, and 436 nm, respectively. The information of surface layers of around

0022–2461/83 $03.00 + .12

micron thickness are expected to be included in the CEM spectra by the additional contribution of secondary electrons emitted by the irradiation of the resonantly scattered γ- (10%) and X-ray (28%).

2. Experimental details

2.1. Preparation of oxalate coatings

Rimmed steel sheets (SPCC-B) were degreased with $20\,g\,l^{-1}$ Fine Cleaner (Nihon Parkerizing Co Ltd) at 75° C for 20 min, washed with water and 15% HCl at room temperature for 5 min, and immersed in $30\,g\,l^{-1}$ oxalate solution at 75° C for 5 min. Stainless steel sheets (SUS 304) were pre-treated by the same procedure as the rimmed mild steel and immersed in $40\,g\,l^{-1}$ oxalate solution containing fluoride and thiosulphate at 80° C for 2 min. After oxalating, the steel sheets were washed with water and dried by air-blowing.

The stretching of the oxalated steel sheets was performed using a rolling machine, spindle oil being used as a lubricant. Oxalated steel and $FeC_2O_4 \cdot 2H_2O$ powder were heat-treated in air, in 95% N_2 + 5% H_2, and in vacuum (10^{-3} torr).

2.2. Measurement of Mössbauer spectra

CEM spectra of oxalated steel surfaces were observed by detecting all electrons emitted by resonant processes with a back-scatter type gas flow counter, under 95% He + 5% CH_4 gas [13]. A 20 mCi ^{57}Co(Rh) source was used. Mössbauer spectra were measured at room temperature and were computer-fitted [14]. The velocity was calibrated by measuring α-iron foil.

3. Results and discussion

3.1. Chemical state of iron in oxalate coating on mild steel

As shown in Fig. 1, doublet peaks of the oxalated iron and magnetically split peaks of the substrate were observed. The isomer shift (I.S.) and quadrupole splitting (Q.S.) of the oxalated iron were 1.17 and 1.75 mm sec^{-1}, respectively, which are consistent with those of $FeC_2O_4 \cdot 2H_2O$ [15].

The crystal structure of $FeC_2O_4 \cdot 2H_2O$ is monoclinic. Each Fe(II) is located at the centre of a distorted octahedron whose vertices are occupied with the oxygen atoms of two water molecules and four coplanar oxygen atoms belonging to two different oxalate groups [16, 17]. The principal axis of the electric field gradient (EFG) of $FeC_2O_4 \cdot 2H_2O$ is considered to be an approximate diagonal which combines oxygens

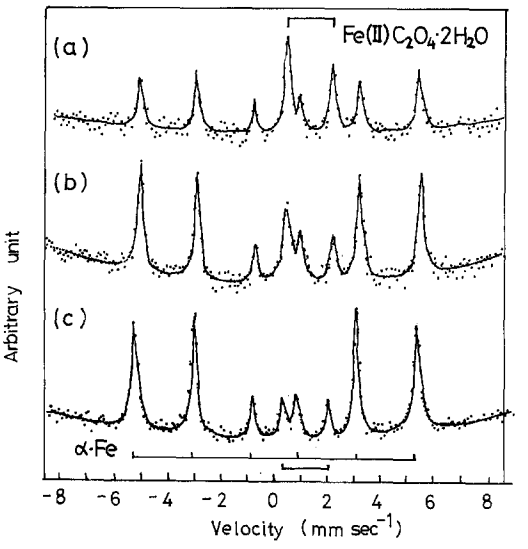

Figure 1 Conversion electron Mössbauer spectra of oxalated mild steel. (a) Unrolled, (b) rolled to 10% reduction, (c) rolled to 30% reduction.

of two water molecules located on opposite sites to each other. It was estimated to be oriented at about 25° to the incident γ-rays, which irradiated perpendicular to the sample surface, according to the calculation made using the asymmetry parameter $\eta = 0.76$ for $FeC_2O_4 \cdot 2H_2O$ [16]. Therefore, the axis of H_2O–Fe–OH_2 of $FeC_2O_4 \cdot 2H_2O$ is, on average, oriented at about 65° to the surface. Gebhart [18] suggested from the similarity of structure between α-Fe and $FeC_2O_4 \cdot 2H_2O$ that the axis of H_2O–Fe–OH_2 in $FeC_2O_4 \cdot 2H_2O$ is parallel to the [1 0 0] axis of α-Fe. The results obtained by Mössbauer study were not consistent with the Gebhart's proposition, which is not always considered to be contradictory because of the polycrystallinity of the deposited $FeC_2O_4 \cdot 2H_2O$ and the substrate material prepared.

3.2. Chemical state of iron in oxalate coating on stainless steel

CEM spectra of the coating on the stainless steel consist of a singlet peak of austenite and doublet peaks of the iron(II) product. The I.S. and Q.S. of the product were 1.18 and 1.71 mm sec^{-1}, respectively. The Q.S. of the iron(II) oxalate, produced on the stainless steel, was slightly smaller than that of $FeC_2O_4 \cdot 2H_2O$ deposited on the mild steel. However, the doublet peaks were assigned to $FeC_2O_4 \cdot 2H_2O$ by the X-ray diffractometric identification. The difference in Q.S. may be due to the formation of the complex

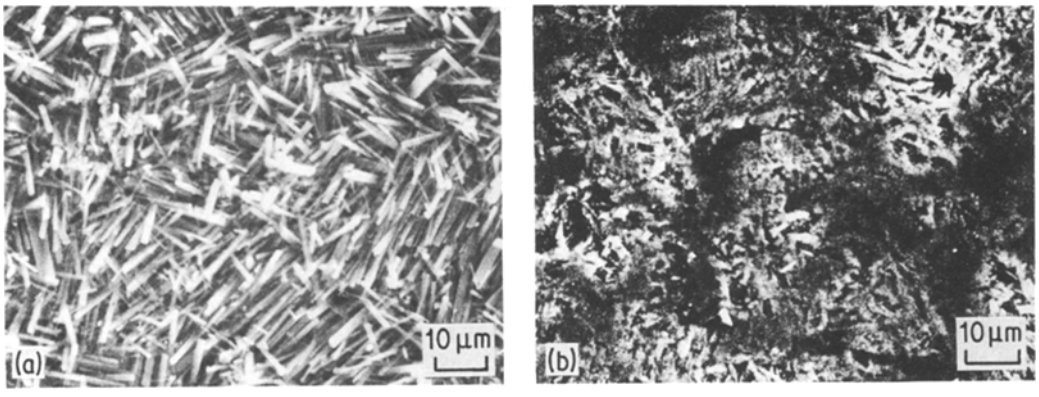

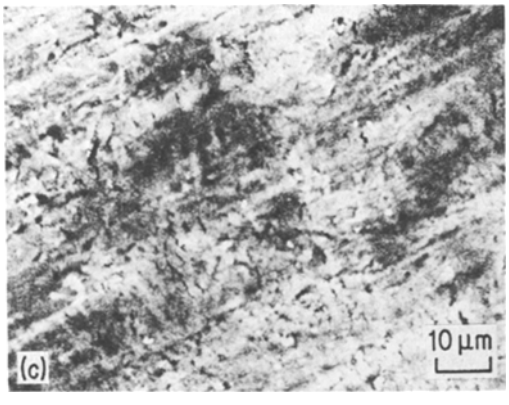

Figure 2 Scanning electron micrographs of oxalated mild steel. (a) Unrolled, (b) rolled to 10% reduction, (c) rolled to 30% reduction.

oxalates of iron, nickel, and chromium, since stainless steel contains such elements as ingredients.

The peak intensity ratio of the doublet peaks of $FeC_2O_4 \cdot 2H_2O$ on the stainless steel was 1.19, which showed that the principal axes of the EFG were oriented at about 45° to the surface. As shown in Figs. 2 and 3, the different columnar shape of the oxalate crystals were arrayed more perpendicular to the surface on the stainless steel than on the mild steel. The oxalate polycrystal is considered to grow up along the four coplanar oxygen atoms.

3.3. Effect of rolling on the iron(II) oxalate coatings

The rolled oxalate coatings were observed by CEMS and the scanning electron microscopy. The columnar shaped crystal of $FeC_2O_4 \cdot 2H_2O$ could not be seen in the photographs of rolled oxalated steels as shown in Figs. 2 and 3. Nevertheless, the presence of $FeC_2O_4 \cdot 2H_2O$ was indicated in CEM spectra. Rolling did not affect the chemical state of iron(II) in the coatings on both mild and stainless steels, but the relative peak intensities of $FeC_2O_4 \cdot 2H_2O$ or $I_{Fe(II)}/(I_{Fe(II)} + I_{Substrate})$ varied.

As shown in Table I, the relative peak intensities of $FeC_2O_4 \cdot 2H_2O$ on the oxalated mild steel before and after rolling by a 0%, 10% and 30% reduction in thickness were 44%, 27% and 12%, respectively. The decrease in the intensities shows that the upper oxalate coating on mild steel has a tendency to be easily scraped off by the rolling.

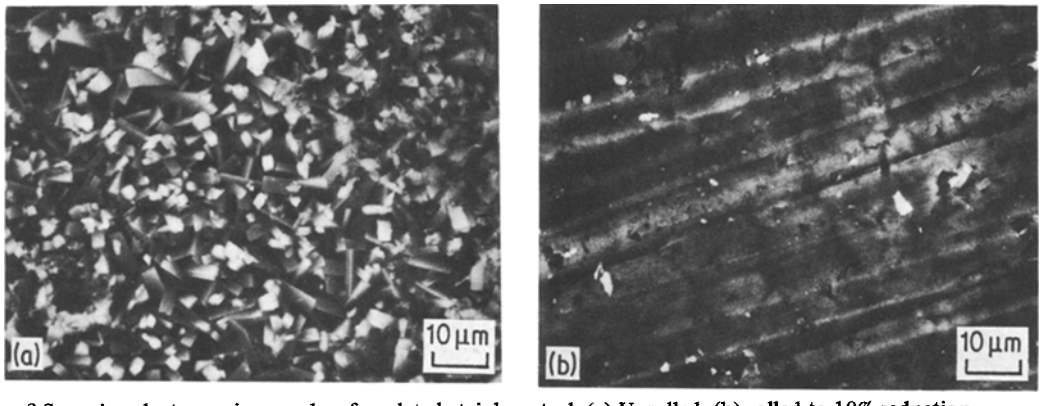

Figure 3 Scanning electron micrographs of oxalated stainless steel. (a) Unrolled, (b) rolled to 10% reduction.

TABLE I Conversion electron Mössbauer parameters of oxalate coatings on mild and stainless steels

Sample	Rolling (% reduction)	I.S. (mm sec^{-1})	Q.S. (mm sec^{-1})	Relative peak intensity of $FeC_2O_4 \cdot 2H_2O$ (%)	Peak ratio
Mild steel	0	1.17 ± 0.02	1.75 ± 0.02	44	1.16‡
	10	1.20 ± 0.02	1.75 ± 0.03	27	1.05‡
	30	1.16 ± 0.03	1.73 ± 0.04	12	1.01‡
Stainless steel (SUS304)	0*	1.18 ± 0.01	1.69 ± 0.02	65	1.16§
	0†	1.20 ± 0.02	1.68 ± 0.03	61	1.19§
	10*	1.19 ± 0.01	1.71 ± 0.01	73	1.17§
	10†	1.19 ± 0.02	1.72 ± 0.02	81	1.19§

*Lower energy electrons detected.
†Higher energy electrons detected.
‡P_{2+5}/P_{1+6} of substrate steel.
§P_1/P_2 of doublet peaks.

On the other hand, the relative peak intensities of $FeC_2O_4 \cdot 2H_2O$ on the oxalated stainless steel increased from 61% to 81% after rolling to 10% reduction in thickness, although the coating weights did not change (about 8.8 g m^{-2}). The oxalate coating was proved to be more adhesive to the stainless steel than to the mild steel.

The increase in relative peak intensity of $FeC_2O_4 \cdot 2H_2O$ by rolling is considered to be due to the fact that the resonantly emitted electrons from the substrate could not pass through the oxalate layers as easily as the unrolled coating because the oxalate layers on steel became fine, tight and dense upon rolling. This evidence is more clearly recognized by observing the depth selective CEM spectra, which can be obtained by detecting emitted electrons of specified energy range.

TABLE II Mössbauer parameters of thermal decomposition products of $FeC_2O_4 \cdot 2H_2O$

Temperature condition (°C)		I.S. (mm sec^{-1})	Q.S. (mm sec^{-1})	H_{in} (kOe)	Products
Room		1.24	1.78		$FeC_2O_4 \cdot 2H_2O$
160	10^{-3} torr air 2 h	1.18	1.63		FeC_2O_4
		0.30	0.70		Fe(III)
230	95% N_2 + 5% H_2 2 h	1.20	2.20		FeC_2O_4
	+ 10^{-3} torr 2 h	0.33	0.75		Fe(III)
230	10^{-3} torr air 4 h	1.16	1.64		FeC_2O_4
		0.62	1.48		Fe(III)
		0.26	0.74		
300	10^{-3} torr air 2 h	0.33	0.75		Fe(III)
300	10^{-3} torr air 30 min	1.1	1.7		FeC_2O_4
		0.4	1.0		Fe(III)
		0.3		492	Fe_3O_4
		0.8		466	
		0.4		490	γ-Fe_2O_3
380	10^{-3} torr air 2 h	0.6		490	γ-Fe_2O_3
380	95% N_2 + 5% H_2 2 h	0		330	α-Fe
		1.1	1.7		FeC_2O_4
		1.1	0.9		Fe(II)
		0.45		490	Fe_3O_4
		0.87		453	
400	air 5 min	0.33	0.74		Fe(III)
		0.42	0.18	490	γ-Fe_2O_3
500	air 10 min	0.50	0.18	522	α-Fe_2O_3

The relative peak intensity of $FeC_2O_4 \cdot 2H_2O$ on the oxalated stainless steel before rolling obtained by detecting lower energy electrons was almost the same as that obtained by detecting higher energy electrons (Figs. 4a and b). This result shows that both the lower and higher energy electrons, resonantly emitted from the steel, can pass through the vacant space and come out of the coating into the detector, and that the energy loss of these electrons during their travel in the oxalate layers is very small. However, the relative peak intensity of $FeC_2O_4 \cdot 2H_2O$, obtained by detecting lower energy electrons emitted from the oxalated stainless steel after rolling by 10% increased more remarkably than that obtained by detecting higher energy electrons Figs. 4c and d. The energy loss for lower energy electrons during their passage through the oxalate layer densified by rolling is more effective than for the higher energy electrons. This difference in the energy loss is responsible for the variation in the relative peak intensity of the oxalate coating before and after rolling.

We have suggested that the degree of adhesion of the coated materials to the substrate is estimated by the intensity ratio among the magnetically split peaks of the substrate [1, 2, 6]. The intensity ratios of P_{2+5}/P_{1+6} for the oxalated mild steels, which were rolled to a 0%, 10% and 30% reduction in thickness, were 1.18, 1.05, and 1.01, respectively, showing the more adhesive fixation of the residual $FeC_2O_4 \cdot 2H_2O$ to the mild steels.

Since the intensity ratio of the mild steel was almost unchanged before and after the oxalate treatment, the degree of adhesion of the oxalate coating to the substrate was not so tight inherently as to cause the change in the magnetic orientation of the domain on the steel surface. The variation of the degree of fixation of the coated oxalate to the substrate and the change of the coating weight by the rolling are considered to result in the variation of the intensity ratio of the magnetically split peaks of the oxalated mild steel.

3.4. Thermal characteristics of oxalate coatings and iron(II) oxalate

The thermal decomposition of $FeC_2O_4 \cdot 2H_2O$ and the physico-chemical properties of the pyrolysis products were studied in detail using DTA, TG and X-ray diffractometry [19]. By utilizing the results reported by several groups on the studies

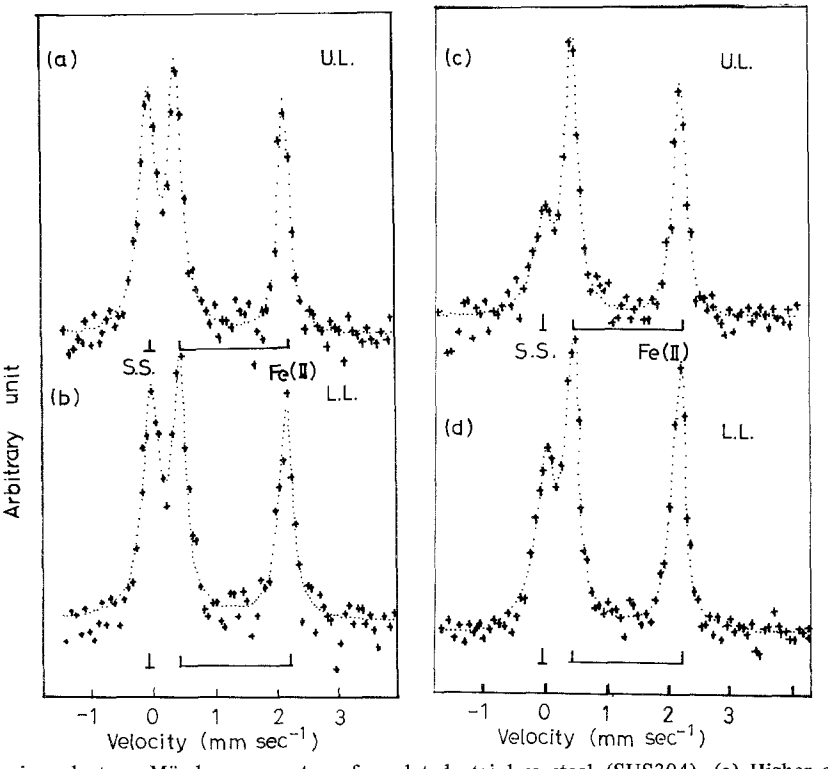

Figure 4 Conversion electron Mössbauer spectra of oxalated stainless steel (SUS304). (a) Higher energy electrons detected (unrolled sample), (b) lower energy electrons detected (unrolled sample), (c) higher energy electrons detected (rolled to 10% reduction), (d) lower energy electrons detected (rolled to 10% reduction).

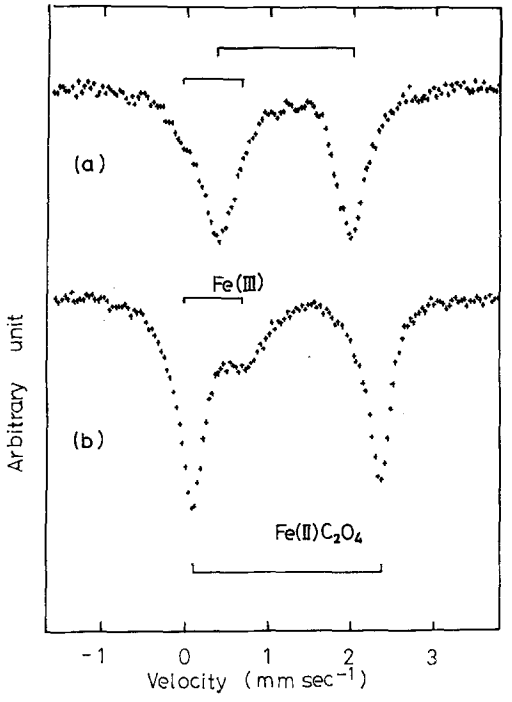

Figure 5 Mössbauer spectra of thermal decomposition products of $FeC_2O_4 \cdot 2H_2O$ heated by two different processes, (a) In vacuum (10^{-3} torr) at 160° C for 2 h, (b) in 95% N_2 + 5% H_2 atomosphere at 230° C for 2 h and then in vacuum (10^{-3} torr) for 2 h.

of thermal decomposition of $FeC_2O_4 \cdot 2H_2O$ in air [20], nitrogen [15] and hydrogen [21] atmospheres by Mössbauer spectrometry, pyrolytic products of $FeC_2O_4 \cdot 2H_2O$ obtained in our experiments were analysed and the Mössbauer data are summarized in Table II.

It is found that FeC_2O_4 transforms to γ-Fe_2O_3 by the oxidation through the intermediate compounds of two paramagnetic species (I.S. = 0.26, Q.S. = 0.74 mm sec^{-1} and I.S. = 0.62, Q.S. = 1.48 mm sec^{-1}) and that $FeC_2O_4 \cdot 2H_2O$ produces the different chemical species of FeC_2O_4 by different ways of dehydration.

In the dehydration process in vacuum (10^{-3} torr) at 160° C for 2 h, the I.S. and Q.S. of the dehydrated FeC_2O_4 were 1.16 and 1.64 mm sec^{-1}, respectively. When $FeC_2O_4 \cdot 2H_2O$ was heated to 230° C to 2 h in 95% N_2 + 5% H_2 atmosphere and then the gas was exhausted rapidly to 10^{-3} torr pressure, the I.S. and Q.S. of the dehydrated FeC_2O_4 were 1.20 and 2.20 mm sec^{-1}, respectively. Therefore, the dehydrated FeC_2O_4 produced by the latter treatment, was assigned to the distorted FeC_2O_4. Mössbauer spectra of these anhydrous products are shown in Fig. 5. A small amount of low-spin iron(III) compound was included in the pyrolysis products as a result of the oxidation by the residual air.

By heating at 300° C for 30 min in 10^{-3} torr, many species were produced, and finally transformed to γ-Fe_2O_3 at 380° C in 2 h, while Fe_3O_4 and α-Fe were produced by heating at 380° C for 2 h in 95% N_2 + 5% H_2 atmosphere as shown in Fig. 6.

$FeC_2O_4 \cdot 2H_2O$ deposited on the stainless steel

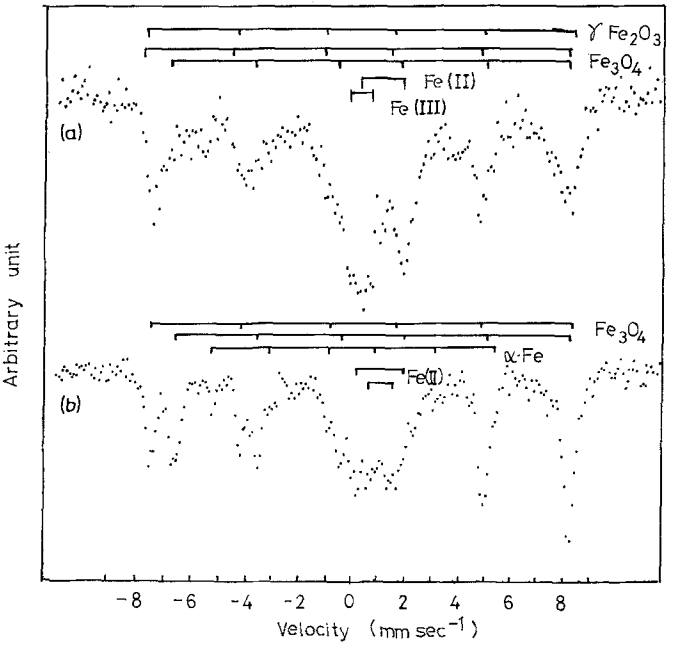

Figure 6 Mössbauer spectra of thermal decomposition products of $FeC_2O_4 \cdot 2H_2O$ heated (a) in 10^{-3} torr air at 300° C for 30 min, (b) in 95% N_2 + 5% H_2 atmosphere at 380° C for 2 h.

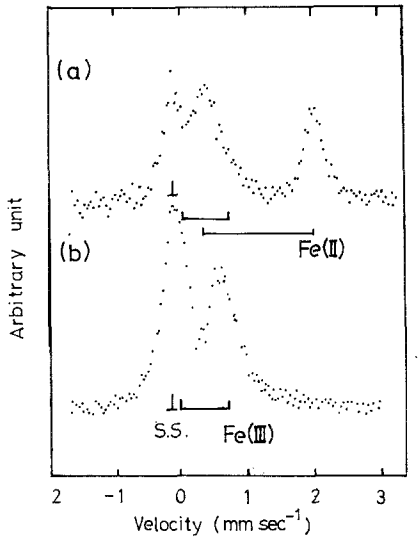

Figure 7 Conversion electron Mössbauer spectra of the heated oxalated stainless steel. (a) In 95% N_2 + 5% H_2 atmosphere at 400° C, (b) in air at 200° C for 1 h.

showed almost the same thermal properties as the neat $FeC_2O_4 \cdot 2H_2O$. When the oxalated stainless steel was heated to 200° C for 1 h in air, only paramagnetic iron(III) compound (I.S. = 0.34, Q.S. = 0.74 mm sec^{-1}) formed as the pyrolysis products. In the CEM spectrum of the oxalated stainless steel heated up to 300° C in 95% N_2 + 5% H_2 atmosphere, FeC_2O_4 was observed in addition to the paramagnetic iron(III) compound as shown in Fig. 7.

The poor resistance to thermal deterioration of the oxalate coating was effectively reconfirmed by CEMS.

Acknowledgement

The authors wish to express their gratitude to chief chemists, Mr S. Sonoda and Mr R. Kojima, Technical Research Laboratory of Nihon Parkerizing Co Ltd, for their helpful discussion on oxalate coatings.

References

1. K. NOMURA, Y. UJIHIRA, Y. MATSUSHITA, R. KOJIMA and Y. SUGAWARA, *Nippon Kagaku Kaishi* (1980) 1371.
2. K. NOMURA and Y. UJIHIRA, Proceedings of the International Conference on the Application of the Mössbauer Effect, Jaipur, India, 14–17 December 1981, Mo-Pi-IN-17.
3. K. NOMURA, Y. UJIHIRA and R. KOJIMA, *Nippon Kagaku Kaishi* (1982) 791.
4. R. KOJIMA, K. NOMURA and Y. UJIHIRA, *Shikizai Kyokaishi* **55** (1982) 365.
5. K. NOMURA, Y. UJIHIRA and R. KOJIMA, *Nippon Kagaku Kaishi* (1982) 87.
6. K. NOMURA and Y. UJIHIRA, *J. Mater. Sci.* **17** (1982) 3437.
7. *Idem, Nippon Kagaku Kaishi* (1982) 1352.
8. A. HANDA and Y. UJIHIRA, *J. Mater. Sci.* in press.
9. A. HANDA, Y. UJIHIRA and I. OKABE, *J. Mater. Sci.* **16** (1981) 1999.
10. Y. UJIHIRA and A. HANDA, *J. de Phys.* **40** (1979) C2-586.
11. KINZOKU HYOMEN GIJUTSU KIYOKAI (ed.), "Kinzoku Hyomen Gijutsu Binran" (Nikkan Kogyo Shimbun, Tokyo, 1970) p. 776.
12. C. FELDMAN, *Phys. Rev.* **117** (1960) 455.
13. Y. UJIHIRA and K. NOMURA, *Bunseki* (1978) 555.
14. B. L. CHRISMAN and T. A. TUMOLILLO, *Computer Phys. Commun.* **2** (1972) 322.
15. M. J. HALSEY and A. M. PRITHARD, *J. Chem. Soc. (A)* (1968) 2878.
16. J. V. De MENEZES and F. Des BARROS, *Phys. Status Solidi (a)* **45** (1978) K139.
17. S. CAVID, *Bull. Soc. Franc. Mineral. Crist.* **82** (1959) 50.
18. M. GEBHARDT, *Farbe und Lack* **74** (1968) 217.
19. H. HASHIMOTO, *Rep. Asahi Glass Found. Ind. Technol.* **37** (1980) 15.
20. A. KRAUCH, G. TOMANDL and G. H. FRISCHAT, *Z. Angew. Phys.* **23** (1967) 419.
21. RAMANI, M. P. SATHYAVATHIAMMA, N. G. PUTTASWAMY and R. M. MALLYA, Proceedings of Nuclear Physics and Solid State Physics Symposium, Ahmedabad, 27–31 December, 1976, Vol. 19C (Solid State Physics) p. 411.

Received 13 September
and accepted 6 October 1982